A Deep-Neural-Network-Based Hybrid Method for Semi-Supervised Classification of Polarimetric SAR Data

Chi Liu[1,2], Wenzhi Liao[1], Heng-Chao Li[2], Shaoguang Huang[1], and Wilfried Philips[1]
[1] *TELIN-IPI, IMEC-Ghent University, Ghent, Belgium*
[2] *Sichuan Provincial Key Laboratory of Information Coding and Transmission*
Southwest Jiaotong University, Chengdu, China

***Abstract*—This paper proposes a deep-neural-network-based semi-supervised method for polarimetric synthetic aperture radar (PolSAR) data classification. The proposed method focuses on achieving a well-trained deep neural network (DNN) when the amount of the labeled samples is limited. In the proposed method, the probability vectors, where each entry indicates the probability of a sample associated with a category, are first evaluated for the unlabeled samples, leading to an augmented training set. With this augmented training set, the parameters in the DNN are learned by solving the optimization problem, where the log-likelihood cost function and the class probability vectors are used. To alleviate the "salt-and-pepper" appearance in the classification results of PolSAR images, the spatial interdependencies are incorporated by introducing a Markov random field (MRF) prior in the prediction step. The experimental results on two realistic PolSAR images demonstrate that the proposed method effectively incorporates the spatial interdependencies and achieves the good classification accuracy with a limited number of labeled samples.**

***Index Terms*—Polarimetric synthetic aperture radar (PolSAR), semi-supervised classification, deep neural networks, remote sensing.**

I. Introduction

Terrain classification is an important application of polarimetric synthetic aperture radar (PolSAR). PolSAR acquires multi-channel data by different combinations of horizontal and vertical polarization, which can provide the useful information about the physical scattering characteristics to accurately identify terrain types [1]. Furthermore, in view of the ability of radar waves to penetrate through clouds, PolSAR can always receive backscattered signals from the ground, facilitating a complete interpretation of areas of interest.

Recently, deep neural networks (DNNs) have become popular in classification tasks of PolSAR images. Many effective methods have been developed based on multilayer autoencoders [2], [3], stacked sparse autoencoders [4], Wishart-autoencoders, Wishart-convolutional-autoencoders [5], and deep convolutional neural networks [6]. These methods leverage the power of DNNs in extracting discriminative features for subsequent supervised classification, leading to a significant improvement on the classification performance over conventional methods. However, in view of both the complicated structures of DNNs and the nature of supervised classification in these DNN-based methods, their performance could be heavily dependent on the amount of training samples.

For the supervised classification of a large-scale PolSAR image, manually labeling a large number of samples for training costs a lot of resources. The use of the limited number of labeled samples presents a challenge to achieve well-trained DNNs, producing unreliable classification results. To address this limitation, a DNN can be learned based on both the labeled samples and the unlabeled samples, leading to semi-supervised classification methods for PolSAR images [7]–[10].

In view of the active imaging mechanism, PolSAR images present a granular noise pattern, which always results in the "salt-and-pepper" appearance in classification results and significantly degrades the classification performance. To alleviate the "salt-and-pepper" effect, the abovementioned semi-supervised methods incorporate the spatial interdependencies. Specifically, the semi-supervised method for feature extraction of PolSAR data constructs the spatial groups by combining neighboring pixels [7]. In addition, the average of the feature vectors (including polarimetric features and the elements from PolSAR data as the entries) for the local pixels is exploited to suppress the "salt-and-pepper" effect [8], [10]. Although the scheme of averaging neighboring pixels incorporates the spatial interdependencies, the resulting features fail to preserve the complete information, leading to the loss of details in the classification results.

In this paper, we propose a semi-supervised DNN-and-MRF-based method (SSDNN-MRF) for PolSAR image classification. Different from [10], which only selects the unlabeled samples with high confidence to enlarge the training set for the DNN, our proposed method exploits all the unlabeled samples. Thus, the operation to select credible samples is eliminated, simplifying the procedure of the semi-supervised classification methods. To this end, the class probability vector associated with each unlabeled sample is first evaluated. In view of the label uncertainty for the augmented data, the training for the DNN is performed based on a log-likelihood function, which can directly deal with the class probability vectors. To

This work was supported in part by the China Scholarship Council, by the FWO project G037115N: Data Fusion for Image Analysis in Remote Sensing, and by the National Natural Science Foundation of China under Grant 61871335. Wenzhi Liao is a postdoctoral fellow of the Research Foundation Flanders (FWO-Vlaanderen, Belgium) and acknowledges its support.

incorporate the spatial interdependencies, the average feature vector associated with a local region is fed to the DNN in the method of Geng *et al.* [10], and is used to represent the spatial group in the graph-based methods [7], [8]. These methods incorporate the spatial interdependencies through the input features. In contrast, the proposed method considers the spatial interdependencies on the labels and leaves the input features untouched, which preserves the complete information of the input features.

II. PRELIMINARIES

A. PolSAR Data and Polarimetric Features

PolSAR acquires multi-channel data by different combinations of transmitting and receiving polarization (e.g., horizontal and vertical polarization). The PolSAR data vector is given by $S = [S_{hh}, S_{hv}, S_{vh}, S_{vv}]^T$, where the superscript T is the transpose operator, and the subscripts h and v indicate the horizontal polarization and the vertical polarization. S_{hv} represents the backscattered signal with horizontal transmitting polarization and vertical receiving polarization. For a reciprocal media, the PolSAR data vector reduces to $S = [S_{hh}, \sqrt{2}S_{hv}, S_{vv}]^T$ in the Lexicographic bases and transforms to $k = 1/\sqrt{2}[S_{hh} + S_{vv}, S_{hh} - S_{vv}, 2S_{hv}]^T$ in the Pauli bases [1]. The multilook PolSAR covariance and coherency matrix are the second-order statistics, which are derived for speckle reduction by averaging n neighboring pixels, i.e., $\mathbf{C} = \frac{1}{n}\sum_{i=1}^{n} S_i S_i^H$ and $\mathbf{T} = \frac{1}{n}\sum_{i=1}^{n} k_i k_i^H$. Here, H is the Hermitian transpose operator.

By factorizing the PolSAR data of these types into the combination of bases associated with physical scattering models, target decomposition (TD) theorems were proposed to extract additional information [1], [11], [12]. The Krogager decomposition analyzes the contribution of the sphere, diplane, and helix targets to the vector S [13]. Based on the multilook polarimetric matrices, the Freeman-Durden decomposition extracts the polarimetric parameters for the volume, double-bounce, and surface scattering [14]. The polarimetric features from TD theorems provide insights into the physical scattering mechanisms over illuminating areas, and facilitate the physical interpretation of PolSAR images.

B. Deep Neural Networks and Backpropagation

A DNN has an architecture of multiple hidden layers, where each hidden layer adopts the outputs from the previous layer as its inputs and yields its outputs by passing a weighted sum of its inputs through a non-linear function [15]. For classification tasks, a DNN aims to map input features to target labels.

To obtain this mapping, a L-layer DNN can be discriminatively trained by solving $\min_{\{\mathbf{W}_l\},\{\mathbf{b}_l\}} C(\mathbf{h}_L, \mathbf{Y})$ [15], where $\mathbf{h}_L$ and $\mathbf{Y}$ respectively indicate the output of the DNN and the underlying discrete labels, and $C(\cdot,\cdot)$ is a cost function to evaluate the discrepancy between them. $\{\mathbf{W}_l\}$ and $\{\mathbf{b}_l\}$ are the weight matrices and the bias vectors used for the feedforward procedure. Specifically, the outputs of the l-th hidden layer $\mathbf{h}_l$ $(l = 1, 2, \cdots, L)$ are evaluated by $\mathbf{h}_l = f_l(\mathbf{Z}_l)$, where $\mathbf{Z}_l = \mathbf{h}_{l-1}\mathbf{W}_l + \mathbf{b}_l$ and the equation of $f_l(\cdot)$ is a non-linear activation function.

The weights $\{\mathbf{W}_l\}$ and the biases $\{\mathbf{b}_l\}$ are commonly learned based on stochastic gradient descent (SGD) and backpropagation [15]. The backpropagation procedure computes the derivatives of the cost function with respect to the weights and the biases. By backpropagating the error derivatives from the output layer to the input layer, the gradients of the outputs over the weights and the biases [see (2) and (3)] are obtained using the chain rule, and SGD can be applied to update $\{\mathbf{W}_l\}$ and $\{\mathbf{b}_l\}$. With N samples involved for the evaluation of the gradients, the backpropagation equations are given by [16]

$$\frac{\partial C}{\partial \mathbf{h}_l} = (\frac{\partial C}{\partial \mathbf{h}_{l+1}} \circ f_l'(\mathbf{Z}_{l+1}))(\mathbf{W}_{l+1})^T, \tag{1}$$

$$\frac{\partial C}{\partial \mathbf{W}_l} = \frac{1}{N} \cdot (\mathbf{h}_{l-1})^T (\frac{\partial C}{\partial \mathbf{h}_l} \circ f_l'(\mathbf{Z}_l)), \tag{2}$$

$$\frac{\partial C}{\partial \mathbf{b}_l} = \frac{1}{N} \cdot sum(\frac{\partial C}{\partial \mathbf{h}_l} \circ f_l'(\mathbf{Z}_l)), \tag{3}$$

where $\circ$ and the superscript T perform the element-wise product and the transpose operation. $f_l'(\mathbf{Z}_l) = \frac{\partial f(\mathbf{Z}_l)}{\partial \mathbf{Z}_l}$, and $sum(\cdot)$ is the summation over the N training samples.

III. METHODOLOGY

In the proposed method for semi-supervised classification of PolSAR images, polarimetric features from TD theorems are collected as the input for a DNN. The input vectors are formulated by stacking 48 features from 10 different TD approaches [17]. This adopted feature set is shown to provide useful information for the effective interpretation of PolSAR images [17].

The proposed method (i.e., SSDNN-MRF) can be implemented by alternatively performing the prediction and the backpropagation procedure. In the prediction step, the augmented training set is achieved and the spatial interdependencies are incorporated. In the subsequent backpropagation procedure, the parameters in the DNN are learned.

A. Augmenting Training Set and Incorporating Spatial Interdependencies

Training set is enlarged by adding all the unlabeled samples, each of which is associated with a class probability vector. To achieve these probability vectors, the L-layer DNN exploits a softmax layer in the rear to perform the classification task. This softmax layer for M categories provides the output $h_L^n = [h_L^{n1}, h_L^{n2}, \cdots, h_L^{nM}]$, where

$$h_L^{ni} = \frac{\exp(\sum_j h_{L-1}^{nj} W_L^{ji} + b_L^i)}{\sum_{k=1}^{M} \exp(\sum_j h_{L-1}^{nj} W_L^{jk} + b_L^k)}. \tag{4}$$

Here, h_{L-1}^{nj} is obtained for an unlabeled sample by the feedforward procedure in the DNN. h_L^{ni} can be interpreted as the probability of a sample belonging to the i-th category.

To incorporate the spatial interdependencies, a MRF prior $p(\widehat{Y}^n = i; \widehat{Y}^{\partial_n}, \beta)$ is imposed on h_L^n, leading to the probability vector $p_n = [p_{n1}, \cdots, p_{nM}]$ as

$$p_{ni} = h_L^{ni} \cdot p(\widehat{Y}^n = i | \widehat{Y}^{\partial_n}; \beta), \tag{5}$$

where h_L^{ni} can be found in (4). $\widehat{Y}^n$ is the estimated label of pixel n, and the estimated labels of its neighbors are denoted by $\widehat{Y}^{\partial_n}$. The MRF prior takes the form of [18]

$$p(\widehat{Y}^n = i|\widehat{Y}^{\partial_n}; \beta) = \frac{\exp(\beta \sum_{m\in\partial_n} \delta(\widehat{Y}^m, i))}{\sum_{j=1}^{M} \exp(\beta \sum_{m\in\partial_n} \delta(\widehat{Y}^m, j))}. \quad (6)$$

Here, $\delta(\widehat{Y}^m, i) = 1$ if and only if $\widehat{Y}^m = i$; otherwise, 0.

The discrete label for each unlabeled sample is determined by identifying the largest element in p_n, i.e., $\widehat{Y}^n = \arg\max_i \ p_{ni}$. Compared with the discrete labels by this criterion, the probability vectors by (5) better preserve the label uncertainty of the augmented data.

B. Learning the DNN

To learn the DNN, the log-likelihood cost function is used in the optimization problem, which allows for the label uncertainty of the augmented data. Given an index set $\mathfrak{L}$ for labeled samples and an index set $\mathfrak{U}$ for augmented data, the optimization problem takes the form of

$$\begin{aligned}\min_{\{\mathbf{W}_l\},\{\mathbf{b}_l\}} \frac{1}{C_0}\Bigg(&- \lambda_{\mathfrak{L}} \sum_{j=1}^{J}\sum_{m=1}^{M} \delta(Y^j, m) \ln h_L^{jm} \\ &- \lambda_{\mathfrak{U}} \sum_{n=1}^{K}\sum_{i=1}^{M} p_{ni} \ln h_L^{ni} + \frac{\epsilon}{2} \parallel \{\mathbf{W}_l\} \parallel_F^2 \Bigg),\end{aligned} \quad (7)$$

where $C_0 = J\lambda_{\mathfrak{L}} + K\lambda_{\mathfrak{U}}$. $\lambda_{\mathfrak{L}}$ and $\lambda_{\mathfrak{U}}$ are the balance parameters for data sets $\mathfrak{L}$ and $\mathfrak{U}$. h_L^{ni} and p_{ni} can be found from (4) and (5). ϵ is a regularization parameter. $\parallel \bullet \parallel_F$ performs the Frobenius norm.

The backpropagation equations for this optimization problem are given in element-wise form by

$$\frac{\partial C}{\partial Z_L^{ni}} = \begin{cases} \lambda_{\mathfrak{L}}(h_L^{ni} - Y^{ni}), & \text{if} \quad n \in \mathfrak{L} \\ \lambda_{\mathfrak{U}}(h_L^{ni} - p_{ni}), & \text{if} \quad n \in \mathfrak{U} \end{cases}, \quad (8)$$

$$\frac{\partial C}{\partial h_l^{ni}} = \sum_k \frac{\partial C}{\partial Z_{l+1}^{nk}} \cdot W_{l+1}^{ik}, \quad (9)$$

$$\frac{\partial C}{\partial Z_l^{ni}} = \frac{\partial C}{\partial h_l^{ni}} \cdot f_l'(Z_l^{ni}), \quad (10)$$

where $l = 1, 2, \cdots, L-1$. We have the partial derivatives as

$$\frac{\partial C}{\partial b_l^i} = \frac{1}{C_0} \sum_{n\in\{\mathfrak{L},\mathfrak{U}\}} \frac{\partial C}{\partial Z_l^{ni}}, \quad (11)$$

$$\frac{\partial C}{\partial W_l^{ik}} = \frac{1}{C_0}\Bigg(\sum_{n\in\{\mathfrak{L},\mathfrak{U}\}} h_{l-1}^{ni} \frac{\partial C}{\partial Z_l^{nk}} + \epsilon W_l^{ik} \Bigg). \quad (12)$$

The biases and the weights can be updated by $(b_l^i)^{(t)} = (b_l^i)^{(t-1)} - \eta \frac{\partial C}{\partial b_l^i}$, and $(W_l^{ik})^{(t)} = (W_l^{ik})^{(t-1)} - \eta \frac{\partial C}{\partial W_l^{ik}}$, where the superscripts $t-1$ and t respectively indicate the previous and current iteration. η is the learning rate.

IV. Experimental Results and Discussion

The propose method is tested based on two realistic PolSAR images, referred to as "Foulum" and "Flevoland". The supervised DNN (SDNN), the SSDNN, and the proposed method adopt the same DNN architecture as the SRDNN method, i.e., two hidden layers with 150 and 40 units.

For data set "Foulum", 1000 samples per category are used for training. The classification maps are presented in Fig. 1. The average values for producer's accuracy, overall accuracy (OA), and kappa coefficient (κ) over 10 independent tests are reported in Table I. The experimental results demonstrate the advantage of the proposed method over the multi-step method (i.e., "SSDNN+MF"). Moreover, the higher OA and κ of the proposed method over the SDNN and the SSDNN reveal that the proposed method benefits from exploiting the unlabeled data and incorporating the contextual information.

For data set "Flevoland", all the compared methods use 1% of the underlying labels (a total of 1564 samples for 15 categories). The experimental results are presented in Fig. 2 and Table II. Since we cannot find the codes for the SNC and the SRDNN, their classification maps and accuracy values are from references [7] and [10]. Compared with the SNC and the SRDNN method, the improved performance has been achieved by the proposed method. The proposed method augments the training set with all the unlabeled data as well as their class probability vectors (instead of discrete labels) so as to consider the label uncertainty. In addition, the proposed method eliminates the procedure of selecting samples, which simplifies the procedure of the semi-supervised method.

TABLE I
Classification Accuracy with the Foulum Data Set.

Class	Producer's Accuracy (%) Supervised DNN	Semi-supervised SSDNN	Semi-supervised SSDNN+MF	Proposed
Water	83.88	95.36	95.56	**96.10**
Coniferous	87.82	85.39	86.74	**88.80**
Winter Wheat	89.59	99.87	**99.93**	99.73
Oats	90.11	98.75	99.16	**99.82**
Rye	56.69	99.50	99.70	**99.90**
Buildings	35.60	87.07	89.45	**91.23**
OA(%)	76.54	90.24	91.29	**92.65**
κ	0.6699	0.8640	0.8785	**0.8971**

V. Conclusion

A DNN-based semi-supervised method has been proposed for PolSAR image classification. All the unlabeled samples as well as the labeled samples were exploited to train the DNN, which overcame the limitation of a small number of labeled samples. The proposed method incorporated the spatial interdependencies through the MRF prior to alleviate the "salt-and-pepper" effect in the classification results. The improved results over the SDNN and SSDNN method have verified the effectiveness of the proposed method in exploiting the unlabeled data and in incorporating the spatial interdependencies. The good performance of the proposed method implies the potential of the DNN in the semi-supervised classification of the PolSAR image.

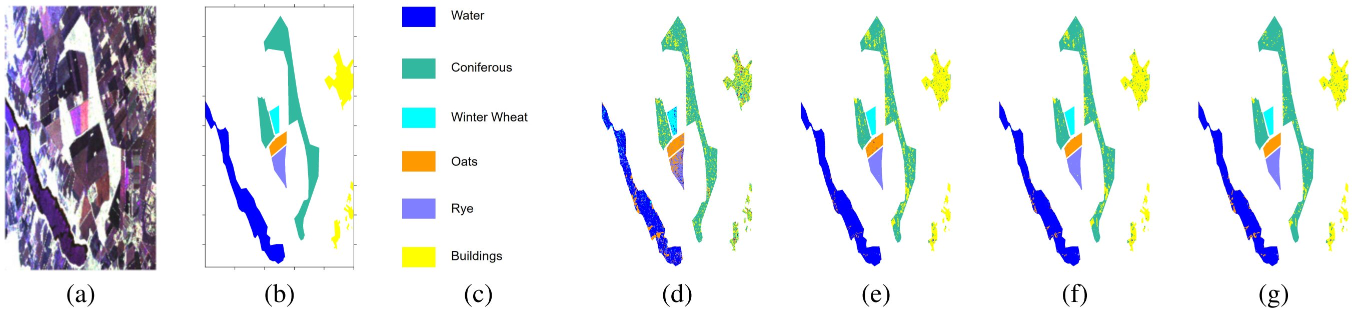

Fig. 1. (a) Pauli RGB image of “Foulum”. (b) Ground truth. (c) Legend. (d) Supervised DNN method. (e) SSDNN method. (f) “SSDNN+MF”. The SSDNN followed by a post-processing step using the mode filter (MF). (g) The proposed method.

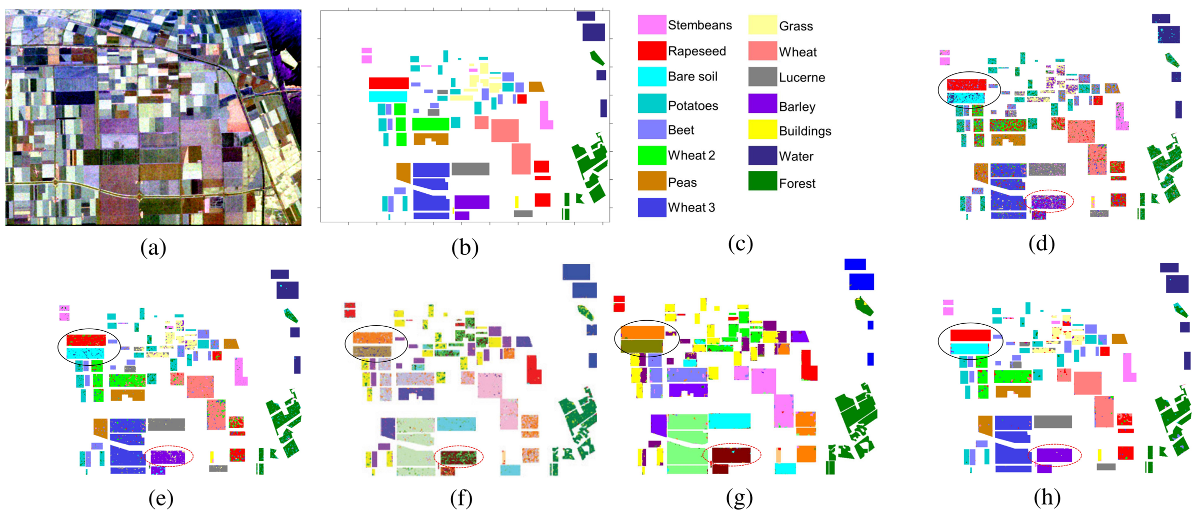

Fig. 2. (a) Pauli RGB image of “Flevoland”. (b) Ground truth. (c) Legend. (d) SDNN method. (e) SSDNN method. (f) SNC method [7]. (g) SRDNN method [10]. (h) The proposed method.

TABLE II
CLASSIFICATION ACCURACY WITH THE FLEVOLAND DATA SET.

Class	Producer's Accuracy (%)				
	SDNN	SSDNN	SNC [7]	SRDNN [10]	Proposed
Stembeans	82.80	92.97	92.35	97.08	**98.09**
Rapeseed	75.98	78.04	69.19	91.81	**94.08**
Bare soil	78.86	93.68	92.11	93.92	**96.51**
Potatoes	64.83	87.84	85.53	94.19	**98.03**
Beet	63.84	92.26	96.66	92.38	**96.91**
Wheat 2	47.66	84.98	71.62	89.65	**90.42**
Peas	75.63	95.90	91.83	94.52	**98.14**
Lucerne	78.01	94.69	92.78	95.55	**97.71**
Wheat 3	85.64	93.96	89.33	97.60	**99.60**
Grass	54.11	83.86	50.54	**87.26**	81.35
Barley	53.73	88.71	64.45	97.57	**99.12**
Wheat	77.41	86.55	83.83	95.52	**96.16**
Buildings	48.04	71.49	73.63	**81.74**	79.47
Forest	76.27	86.33	90.44	**97.31**	93.68
Water	96.71	99.26	97.60	99.53	**99.79**
OA(%)	73.28	89.45	84.64	94.66	**95.99**
κ	0.7086	0.8851	-	0.9418	**0.9563**

REFERENCES

[1] J.-S. Lee and E. Pottier, *Polarimetric Imaging: From Basics to Applications*, CRC Press, Boca Raton, FL, 2009.

[2] B. Hou, H. Kou, and L. Jiao, “Classification of polarimetric SAR images using multilayer autoencoders and superpixels,” *IEEE J. Sel. Topics Appl. Earth Observ. Remote Sens.*, vol. 9, no. 7, pp. 3072–3081, July 2016.

[3] H. Liu, S. Yang, S. Gou, D. Zhu, R. Wang, and L. Jiao, “Polarimetric SAR feature extraction with neighborhood preservation-based deep learning,” *IEEE J. Sel. Topics Appl. Earth Observ. Remote Sens.*, vol. 10, no. 4, pp. 1456–1466, Apr. 2017.

[4] L. Zhang, W. Ma, and D. Zhang, “Stacked sparse autoencoder in PolSAR data classification using local spatial information,” *IEEE Geosci. Remote Sens. Lett.*, vol. 13, no. 9, pp. 1359–1363, Sep. 2016.

[5] W. Xie, L. Jiao, B. Hou, W. Ma, J. Zhao, S. Zhang, and F. Liu, “POLSAR image classification via Wishart-AE model or Wishart-CAE model,” *IEEE J. Sel. Topics Appl. Earth Observ. Remote Sens.*, vol. 10, no. 8, pp. 3604–3615, Aug. 2017.

[6] S. W. Chen and C. S. Tao, “PolSAR image classification using polarimetric-feature-driven deep convolutional neural network,” *IEEE Geosci. Remote Sens. Lett.*, vol. 15, no. 4, pp. 627–631, Apr. 2018.

[7] H. Liu, D. Zhu, S. Yang, B. Hou, S. Gou, T. Xiong, and L. Jiao, “Semisupervised feature extraction with neighborhood constraints for polarimetric SAR classification,” *IEEE J. Sel. Topics Appl. Earth Observ. Remote Sens.*, vol. 9, no. 7, pp. 3001–3015, July 2016.

[8] H. Liu, S. Yang, S. Gou, P. Chen, Y. Wang, and L. Jiao, “Fast classification for large polarimetric SAR data based on refined spatial-anchor graph,” *IEEE Geosci. Remote Sens. Lett.*, vol. 14, no. 9, pp. 1589–1593, Sep. 2017.

[9] B. Hou, Q. Wu, Z. Wen, and L. Jiao, “Robust semisupervised classification for PolSAR image with noisy labels,” *IEEE Trans. Geosci. Remote Sens.*, vol. 55, no. 11, pp. 6440–6455, Nov. 2017.

[10] J. Geng, X. Ma, J. Fan, and H. Wang, “Semisupervised classification of polarimetric SAR image via superpixel restrained deep neural network,” *IEEE Geosci. Remote Sens. Lett.*, vol. 15, no. 1, pp. 122–126, Jan. 2018.

[11] S. R. Cloude and E. Pottier, “A review of target decomposition theorems

in radar polarimetry," *IEEE Trans. Geosci. Remote Sens.*, vol. 34, no. 2, pp. 498–518, Mar. 1996.

[12] R. Touzi, "Target scattering decomposition in terms of roll-invariant target parameters," *IEEE Trans. Geosci. Remote Sens.*, vol. 45, no. 1, pp. 73–84, Jan. 2007.

[13] E. Krogager, "New decomposition of the radar target scattering matrix," *Electron. Lett.*, vol. 26, no. 18, pp. 1525–1527, Aug 1990.

[14] A. Freeman and S. L. Durden, "A three-component scattering model for polarimetric SAR data," *IEEE Trans. Geosci. Remote Sens.*, vol. 36, no. 3, pp. 963–973, May 1998.

[15] Yann LeCun, Yoshua Bengio, and Geoffrey Hinton, "Deep learning," *nature*, vol. 521, pp. 436–444, 2015.

[16] H. Wang and D. Yeung, "Towards Bayesian deep learning: A framework and some existing methods," *IEEE Trans. Knowl. Data Eng.*, vol. 28, no. 12, pp. 3395–3408, Dec. 2016.

[17] M. Tao, F. Zhou, Y. Liu, and Z. Zhang, "Tensorial independent component analysis-based feature extraction for polarimetric SAR data classification," *IEEE Trans. Geosci. Remote Sens.*, vol. 53, no. 5, pp. 2481–2495, May 2015.

[18] S. P. Chatzis and G. Tsechpenakis, "The infinite hidden Markov random field model," *IEEE Trans. Neural Netw.*, vol. 21, no. 6, pp. 1004–1014, June 2010.